Virchows Archiv A Pathol Anat (1993) 423:121–129

Virchows Archiv A
Pathological Anatomy and Histopathology

Widening of capillary neck and alteration of extracellular matrix ultrastructure in diabetic rat glomerulus as revealed by computer morphometry and improved tissue processing

Isao Shirato[1], Tatsuo Sakai[2], Mitsumine Fukui[1], Yasuhiko Tomino[1], Hikaru Koide[1]

[1] Division of Nephrology, Department of Medicine, Juntendo University, School of Medicine, Tokyo, Japan
[2] Department of Anatomy, Juntendo University, School of Medicine, Tokyo, Japan

Received March 2, 1993 / Received after revision May 13, 1993 / Accepted May 14, 1993

Abstract. Morphological and morphometric studies of glomeruli were carried out in streptozotocin-induced diabetic rats using improved tissue processing and computerized morphometry. Increased mesangial matrix, occupying the enlarged diabetic mesangium, contained an abundance of dark granular material in addition to the microfibrils which were usually found in the control glomeruli. In the diabetic glomeruli, the lamina densa was thick and heterogeneous showing a dense layer both on its epithelial and endothelial aspects, and the lamina rara externa contained more fibrils than in control rats. Detailed estimation of the absolute values of the various compartments of the diabetic glomeruli by using perfusion-fixed materials and a computer-assisted digitizer revealed that the volume and surface area of the mesangium were increased more extensively than those of the capillary; the enlargement of the mesangial-capillary interface area was the most pronounced among the morphometric changes of the diabetic glomeruli; and that the moderate increase in capillary volume was associated with an increased radius. Our quantitative results showed that capillaries in the diabetic glomeruli had an extensively wider neck which may be the first sign of structural damage to the glomerular tuft.

Key words: Ultrastructure – Morphometry – Diabetic nephropathy – Rat

Introduction

Diabetic nephropathy produces significant structural changes in the glomeruli which develop progressively. Morphological and histochemical investigations have revealed various characteristic structural and compositional changes and increased thickness of the glomerular basement membrane (GBM) and widening of the mesangium represent the initial structural changes in diabetic glomeruli (Mauer et al. 1981; Walker et al. 1992). The mesangium and the GBM change the composition of their structural proteins and accumulate circulating macromolecules non-specifically (Tisher and Hostetter 1989; Nerlich and Schleicher 1991; Kim et al. 1991). Stereological studies of diabetic nephropathy have revealed that mesangial expansion has an inverse correlation with creatinine clearance (Mauer et al. 1984) and that glomerular filtration rate is closely associated with the glomerular filtration surface (Østerby et al. 1988). These initial structural and compositional changes are thought to have pathological significance, or at least to indicate the degree of disease progression.

Experiments using an animal model of diabetic nephropathy have two advantages over those on human material despite the fact that the animal model does not develop severe glomerular lesions such as nodular glomerulosclerosis. First, the therapeutic effect of various manoeuvres can be evaluated; as an example the control of the blood sugar level and administration of an angiotensin converting enzyme inhibitor or aldose reductase inhibitor are reported to prevent the progression of diabetic nephropathy in part (Steffes et al. 1980; Mauer et al. 1989; Fujiwara et al. 1992). Second, the kidneys of an experimental animal can be fixed by perfusion which is necessary for reasonable preservation of the glomerular structure and geometry, allowing the absolute size of the various compartments of the glomeruli to be estimated. This advantage has been fully exploited in volume-expanded and volume-depleted rats (Elger et al. 1990) and in the isolated perfused kidney (Sakai et al. 1992).

In this study, we employed several technical improvements to visualize and quantitate the structural changes in the glomeruli of diabetic rats. Perfusion-fixation with a pressure-control apparatus minimizes the alteration of glomerular geometry during fixation. By combining tannic acid and uranyl acetate staining, followed by dehy-

Correspondence to: H. Koide, Division of Nephrology, Department of Medicine, Juntendo University, School of Medicine, 2-1-1 Hongo, Bunkyo-ku, Tokyo 113, Japan

dration in cold acetone, the extra- and intracellular filamentous structures of the glomeruli have been visualized more clearly than by the conventional method using osmium tetroxide.

Materials and methods

Male Sprague-Dawley rats (7 weeks of age and about 200 g body weight at the start of the experiment) were rendered diabetic by i.v. injection of streptozotocin (STZ) (65 mg/kg body weight; Upjohn, Kalamazoo, Mich., USA). One week after injection, the animals with a blood glucose level above 300 mg/dl were selected for the present study ($n=8$). Age-matched rats received i.v. injection of saline were used as controls ($n=8$). Throughout the experiments, the rats had free access to a normal rat chow and tap water.

At 12 or 24 weeks after induction of diabetes, the rats ($n=4$ in each diabetic and control groups) were anaesthetized by i.p. injection of pentobarbital (Nembutal, Abbott Laboratory, Ill., USA) 25 km/kg body weight. The kidneys were fixed by arterial perfusion as described by Kaissling and Kriz (1982). Briefly, after opening the abdominal cavity, the abdominal aorta was cannulated with a retrograde catheter, and perfused by a fixative without preflushing with a perfusion apparatus (Kosaka Laboratory, Tokyo, Japan) operated at a pressure of 220 mmHg for 3 min. A fixative contained 2% glutaraldehyde in 0.1 M cacodylate buffer at pH 7.4.

For light microscopic examination, the right kidney was embedded in paraffin. Sections (3 μm) were cut halfway between the two poles of the kidney along the corticopapillary axis and stained with periodic-acid Schiff.

For electron microscopic observations, small pieces of cortical tissue from the left kidney were processed by a cold-dehydration technique for visualization of extracellular matrix and intracellular fibrillar structures (Sakai and Kriz 1987). After brief treatment with 0.1% osmium tetroxide, the blocks were stained en bloc with 1% tannic acid and uranyl acetate successively. The blocks were then dehydrated in graded series of acetone at gradually decreasing temperature down to −30° C and embedded in Epon 812. Ultrathin sections of the superficial cortex vertical to the kidney surface were cut with diamond knives, stained with uranyl acetate and lead citrate, and examined in a Hitachi H-500 electron microscope.

For morphometric analysis with electron microscope, cortical slices of the left kidney were made from a different part of the left kidney and were cut into small pieces which were post-fixed in 1% osmium tetroxide, dehydrated in graded series of ethanol and embedded in Epon 812. Semi-thin sections (0.5 μm thick) vertical to the kidney surface were cut from at randomly selected blocks of tissue and stained with toluidine-blue. From blocks contained superficial cortex, glomeruli at least one tubular diameter from the section edge, which showed maximum radius and did not intersect the vascular and/or urinary pole, were selected for thin sectioning. The entire glomerulus was photographed in a Hitachi H-500 electron microscope at a magnification of ×1500 and photomontage of ×2700 was made. Three glomeruli per animal and thus a total of 12 glomeruli per group, were photographed.

Absolute sizes of the glomerular tuft and of its various compartments were estimated on the basis of combination of measurements both on the paraffin sections and on the electron micrographs.

On paraffin sections, the mean glomerular tuft volume [$V(T)$] were determined in four animals of each group. The measurements were carried out on the superficial and midcortical glomeruli located at a distance less than 500 μm from the renal capsule. In each animal, the cross sectional areas of 100 random glomerular tuft profiles were measured. This was done by moving the sections under the microscope parallel to the kidney surface and sampling all glomerular profiles which appeared in the visual field. The sections were spaced at least 150 μm apart to avoid measuring the same glomerulus repeatedly. The measurements were made employing a semi-automatic image analysis system (IBAS, Carl Zeiss, Oberkohen, Germany) connected to a Zeiss photomicroscope. Outlines of the profiles, as viewed on a video monitor, were traced on a digitizing tablet at a magnification of ×1000. The glomerular tuft area was defined as the minimal convex polygon circumscribing all tuft components (capillaries, mesangium, and podocytes) and the narrow urinary space entrapped in the tuft area. An independent estimate of glomerular tuft volume, $V(T)$, in each of the animals was calculated from the mean tuft area, $A(T)$ (100 random profiles each), using the formula; $V(T)=\beta/K\cdot A(T)\wedge(3/2)$, where β (=1.38) represents a shape coefficient for spheres and K (=1.1) is a distribution co-efficient (Hirose et al. 1982; Weibel 1979). As the procedure for paraffin embedding causes shrinkage of the renal tissue by approximately 0.52 cm ∧ 3/g kidney (Bankir et al. 1988), the values of the glomerular volume reported were corrected for shrinkage.

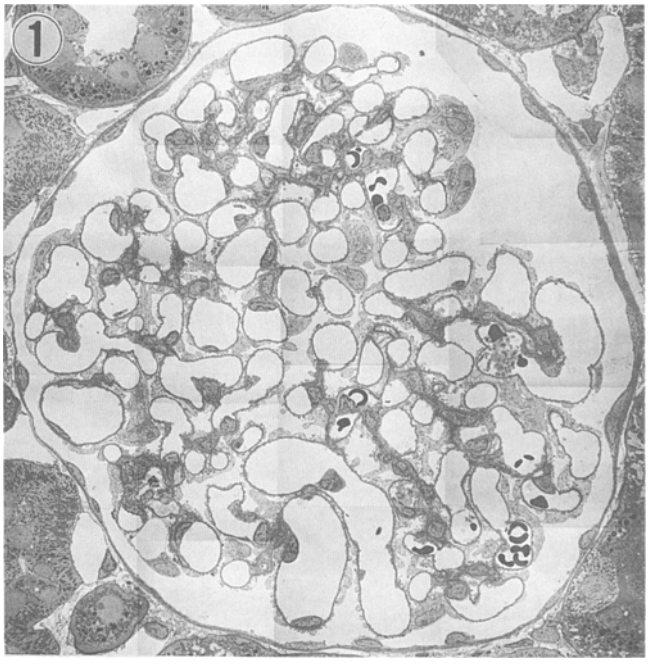

Fig. 1. Electron microscopic photomontage of a 24-week-old control glomerulus, prepared for morphometry

For stereological analysis of tuft components, electron microscopic photomontages were made at a final magnification of ×2700 (Fig. 1). Field areas and outline lengths of various compartments of the glomerular tuft were measured using digitizer and Cosmozone software (Nikon, Tokyo). To facilitate tracing of structures with digitizer mouse, the course of the glomerular basement membrane (GBM), the junctions between the different subdomains of the GMB, and the mesangial-capillary interface were delineated with coloured marking pens on the micrograph before measuring. A total of 12 glomeruli were investigated per group, 3 glomeruli per animal. As a basis of further calculations, the following parameters were determined.

The length of the entire GBM and of several sub-domains of the GBM were determined (Fig. 2). Two main sub-divisions are the pericapillary and the perimesangial GBM, which are demarcated from each other by the mesangial angles. The pericapillary subdomains is bordered by the podocyte and endothelial layer, the perimesangial sub-domain by podocyte and the mesangium. We measured the entire GBM and the pericapillary GBM; the perimesangial GBM was obtained from the difference between the two. In addition, two sub-domains of the pericapillary GBM were separately recorded: the sub-domain facing the attenuated, fenestrated endothelium (defined as "filtering" GBM), and the GBM subdomain facing endothelial cell bodies (defined as "endothelial"

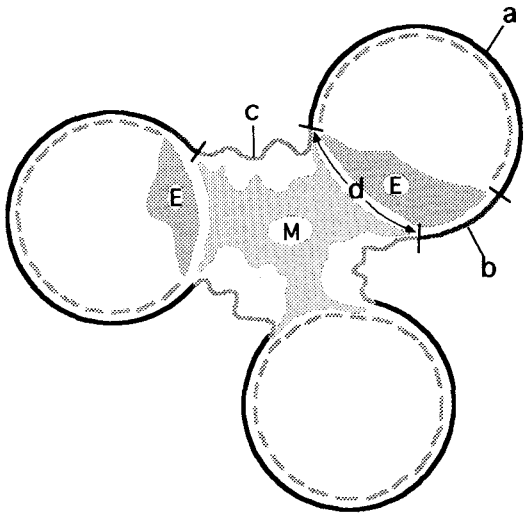

Fig. 2. Schematic representation of different segments of glomerular tuft. Abbreviations: a, filtering GBM; b, endothelial GBM; (a+b, pericapillary GBM); c, perimesangial GBM; d, mesangial-capillary interface; M, mesangial cell; E, endothelial cell

GBM) (Fig. 2). By area analysis, the entire tuft area (corresponding to the convex polygon determined light microscopically), the GBM-included area, and the capillary luminal area including endothelium were measured. The GBM included area comprises all tuft components lying inside the GBM. By subtracting the capillary luminal area from the GBM-included area, we obtained the area consisting of mesangium.

The surface density of the GBM, Sv(GBM), or its sub-domains, was calculated according to the formula $Sv(\mathrm{x}/glom)=4/\pi B_A(\mathrm{GMB}/Glom)$, where B_A was the length of the GBM (or some sub-domains of it) divided by the GBM-included area of the same glomerular profile. Volume densities, Vv, of tuft compartment per unit GBM-included volume were also determined.

The average diameter of capillaries (d) was derived from the average cross-sectional area of capillaries (A) as $d=2(A/\pi)^{1/2}$. On the basis of the cylindrical structure of capillaries, A = V/L was estimated by $A=Vv$(capillary lumen/GBM-included volume)/Lv(capillary length/GBM-included volume). Lv, the length per unit volume, was determined by $2\times N_A$, where N_A was the number of capillary profiles per unit GBM-included area.

Absolute values of tuft components per glomerulus were calculated as the product of the relative structural quantities (surface and volume densities evaluated in transmission electron mciroscopy) and absolute tuft volumes determined by light microscopy and corrected for shrinkage, that is to say, for absolute surface area of GBM

S(GBM) = Sv(GBM/GBM-included volume)
$\times Vv$(GBM-included volume/tuft polygon)
$\times V$(tuft polygon) mm^3 (from light microscopy).

The GBM thickness was measured directly with a scale magnifying glass of $\times 7$ magnification. The width between inner sites of epithelial and endothelial cell membrane in the peripheral capillary wall was measured at 1 μm intervals at the area showing orthogonal cross-sections in a whole glomerulus. Orthogonal cross-sections were determined where the areas of the epithelial and endothelial cytoplasmic membrane were clearly visible. Average numbers of measurement per glomerulus were 150–200 points in 30–40 peripheral capillary walls each rat.

At electron microscopic level, average values based on the measurement of 3 individual glomeruli were determined for each animal.

Blood and urine were collected before sacrifice at the end of 12 or 24 weeks after induction of diabetes. Blood was drawn from the tail vein and glucose measured by an *o*-toluidine blue method (Hyvarinen and Nikkila 1962). Serum creatinine was measured by Jaffe method. The rats were then individually housed in metabolic cages for collection of 24 h urine samples. Urinary protein was measured by Tonein TP Kit (Coomassie brilliant blue G-250, Otsuka Pharmacy, Tokyo, Japan) (Nakamura et al. 1991).

Results are expressed as the median and the mean ± SE. Group differences were assessed by Mann-Whitney U-test (StatView 4.0, Abacus Consepts, Berkeley, Calif., USA). Significant difference was considered to be $p<0.05$.

Results

The body weight and biochemical data indicate that diabetic nephropathy had developed by 12 weeks and had progressed by 24 weeks after the injection of STZ (Table 1). The relative loss of body weight in the diabetic rats amounted to about 50% in the 12 week old group and to about 40% in the 24 week old group, due to slow weight gain in the diabetic animals. The average blood glucose of the diabetic rats was persistently greater than 500 mg/dl. There was no significant difference in the serum creatinine levels between the control and diabetic rats. A significantly increased excretion of urinary protein was noted in the 12-week-old diabetic rats and was even greater in the 24-week-old diabetic rats.

Structural changes in the diabetic glomeruli, which consisted of an enlargement of the mesangium and a thickening of the GBM, were observed in both the 12- and 24-week-old diabetic rats, the extent of the changes being greater in the 24-week-old diabetics. The enlargement of the mesangium is visible at a low power magnification as a widening of the axial region of the tuft (Fig. 3). In the mesangium, the mesangial matrix accumulated to expand the perimesangial GBM to Bowman's space. The perimesangial GBM of the diabetic glomeruli has lost most of its infolding seen in the normal glomeruli. The mesangial-capillary interface was widened from its normal slim configuration and the capil-

Table 1. Body weight and biochemical data

	12W C	12W DM	24W C	24W DM
Body weight (g)	530 (532 ± 6)	288 (284 ± 14.5)[a]	568 (567 ± 8.5)	343 (345 ± 10.5)[b]
Blood glucose (mg/dl)	165 (168 ± 2.5)	668 (662 ± 14.5)[a]	168 (165 ± 5.5)	582 (579 ± 10)[b]
Serum creatinine (mg/dl)	0.9 (0.9 ± 0.1)	1.0 (1.0 ± 0.15)	1.0 (1.0 ± 0.1)	1.1 (1.1 ± 0.1)
Urine protein (mg/day)	9.3 (9.1 ± 0.6)	15.8 (15.4 ± 1.1)[a]	15.3 (15.6 ± 2.9)	47.8 (47.3 ± 6.7)[b]

Data are expressed as the median and (the mean ± SE) [a] different from 12W C, $p<0.01$, [b] different from 24W C, $p<0.01$

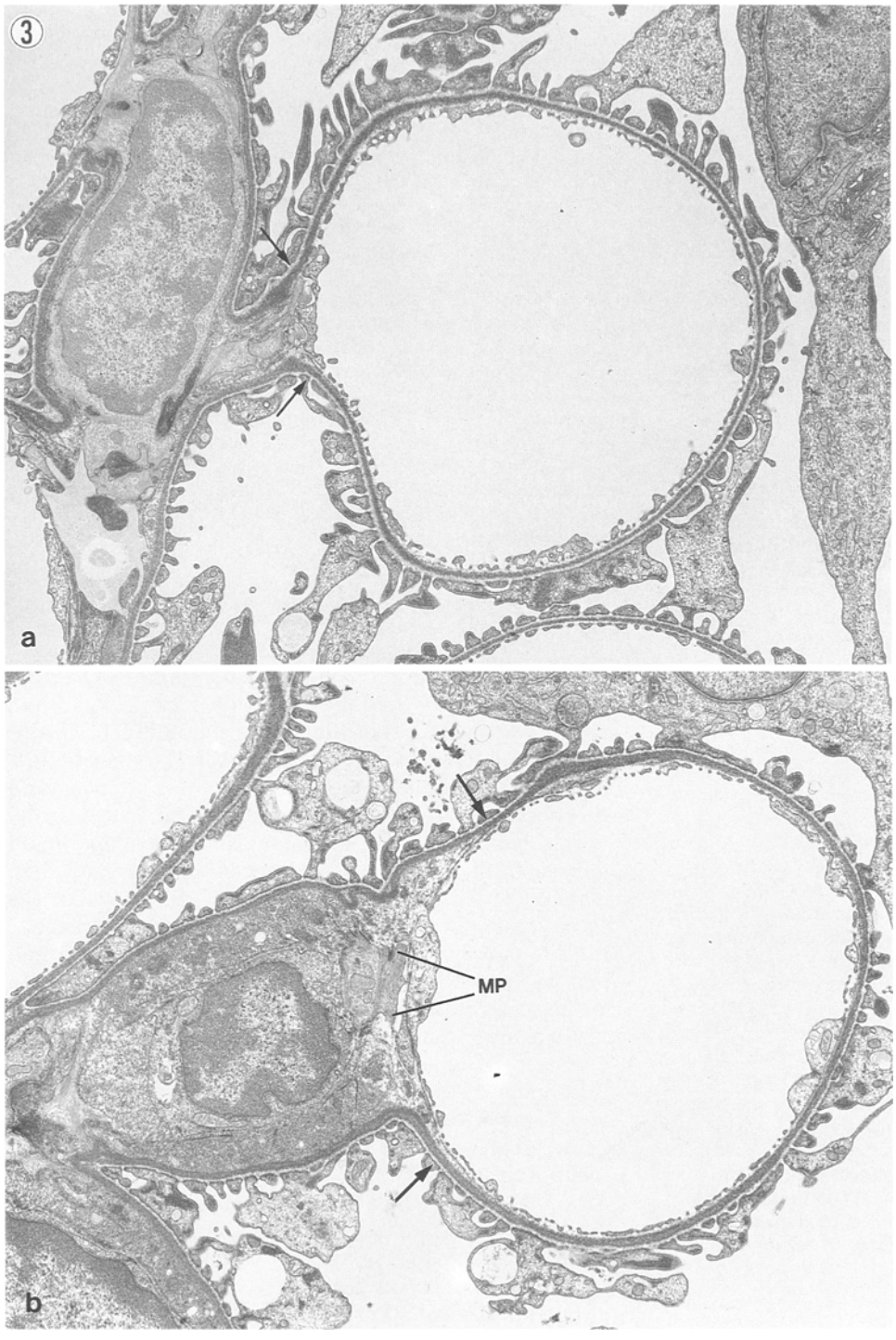

Fig. 3a, b. Profiles of a glomerular capillary and the adjoining mesangium from a kidney of (**a**) control and (**b**) 24 week diabetic rat. **a** The GBM along with the epithelial foot processes deviates from its pericapillary course at the mesangial angle (indicated by *arrows*) to a perimesangial course. The perimesangial GBM covers mesangial cells with the interposition of a small amount of mesangial matrix. **b** The glomerular capillary wall in the diabetic rat shows an increased thickness in the GBM. In the mesangium, the mesangial matrix is increased and widens the distance between the mesangial cells and the perimesangial GBM. Mesangial cell processes (MP) between mesangial angles (indicated by *arrows*) have lost their contact with the GBM. Transmission electron micrograph (TEM) **a**, **b** $\times 8640$

laries had a wide neck in the diabetics. Both ends of the mesangial-capillary interface, namely the mesangial angles, were more distant from each other in the diabetics than in the controls.

In the widened mesangial-capillary interface of the diabetic glomeruli, mesangial cell processes occupied, in most cases, only a part of the distance between the opposing mesangial angles (Fig. 3). Stretched-out processes bridging the mesangial angles were only occasionally encountered in the diabetics (Fig. 4). However, the mesangial cells in the controls frequently sent out tongue-like progresses which made contact with the GBM at the mesangial angles.

The increased mesangial matrix of the diabetic rats appeared heterogeneous with dense and light portions (Fig. 5). In the high power view, the matrix in the diabetics contained an abundance of dark granular material in addition to microfibrils which were usually found in the controls. The dark granular material accumulated more densely in the dense portions of the matrix.

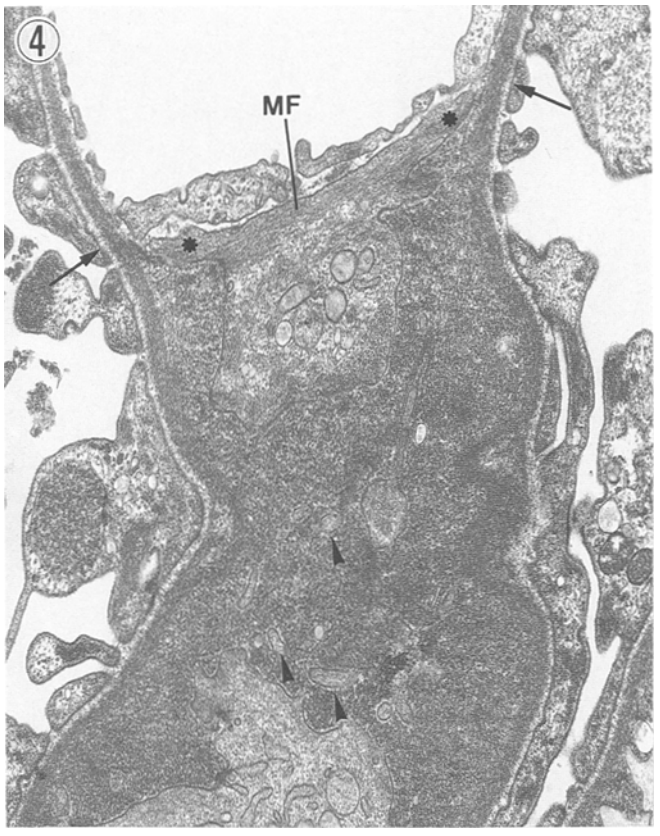

Fig. 4. The mesangium from a kidney of a 24 week diabetic rat. The increased mesangial matrix fills the major part of mesangium. Many mesangial processes (*arrowheads*) have lost their contact with the GBM, and are embedded in the mesangial matrix. In the tongue-like projections (*) at the mesangial-capillary interface which maintain contact with the GBM, a bundle of microfilaments (MF) anchors the two mesangial angles (*arrows*). TEM ×27000

The density of the lamina densa in the diabetic glomeruli was heterogeneous and revealed dense sub-layers both on its epithelial and endothelial aspects (Fig. 6). The contour of the epithelial side of the lamina densa was undulated compared with the straight outline of the endothelial side. In the lamina rara externa, fine fibrils which connect the lamina densa with epithelial foot processes were more abundant in the diabetic rats than in the control rats.

Morphometric data (summarized in Table 2 and Fig. 7) revealed that the enlargement of the glomerulus in the diabetics was accompanied by an increase in both the tuft volume and the tuft surface area. The enlargement was more extensive in the mesangium than in the capillary, and less pronounced in the 12 week diabetics than in the 24 week diabetics.

The total GBM area increased by 7% in the 12 week diabetics and 10% ($p<0.05$) in the 24 week diabetics. The increase was brought about mainly by an enlargement of the perimesangial GBM area, while the pericapillary GBM area (filtering GBM area + endothelial GBM area) was almost unchanged. The increase in the perimesangial GBM area (24% in the 12-week-old and 44%, $p<0.01$, in the 24-week-old diabetes) may have been partly caused by a expansion of mesangial matrix.

The moderate increase in the capillary volume was associated with an increase in the capillary surface area (filtering GBM area + endothelial GBM area + mesangial-capillary interface area). Among the sub-domains of the capillary surface area, the mesangial-capillary interface area was the most remarkably enlarged. The enlargement of the mesangial-capillary interface area was most pronounced among the geometric changes of the diabetic glomeruli, by about 60% ($p<0.01$) in the 12

Table 2. Morphometric data of control and diabetic rat glomeruli

	12W C	12W DM	24W C	24W DM
Volume (10^6 μm^3)				
Glomerular volume				
Tuft	1.534 (1.534±0.013)	1.698 (1.686±0.007)[a]	1.682 (1.671±0.028)	2.085 (2.086±0.011)[c]
GBM included	0.941 (0.954±0.015)	0.984 (0.977±0.012)	0.979 (0.988±0.019)	1.258 (1.257±0.027)[c]
Capillary volume	0.831 (0.834±0.009)	0.811 (0.800±0.015)	0.880 (0.881±0.020)	1.022 (1.015±0.028)[c]
Mesangial volume	0.114 (0.119±0.007)	0.175 (0.177±0.004)[a]	0.106 (0.106±0.006	0.240 (0.241±0.004)[c]
Area (10^6 μm^2)				
Total GBM	0.382 (0.375±0.008)	0.408 (0.401±0.012)	0.393 (0.386±0.013)	0.432 (0.432±0.006)[d]
Filtering GBM	0.263 (0.261±0.005)	0.275 (0.272±0.008)	0.283 (0.275±0.011)	0.288 (0.288±0.003)
Endothelial GBM	0.048 (0.043±0.007)	0.051 (0.045±0.007)	0.033 (0.034±0.004)	0.029 (0.028±0.003)
Perimesangial GBM	0.066 (0.071±0.004)	0.082 (0.084±0.003)	0.076 (0.076±0.007)	0.110 (0.116±0.007)[c]
Mes.-Cap. interface	0.043 (0.045±0.002)	0.069 (0.069±0.002)[a]	0.057 (0.058±0.004)	0.115 (0.115±0.002)[c]
Capillary diameter (μm)	8.30 (8.46±0.11)	8.76 (8.82±0.14)[b]	8.97 (8.93±0.15)	9.45 (9.49±0.15)[d]
Capillary length (10^3 μm)	15.61 (15.36±1.5)	13.52 (13.21±0.57)	14.25 (14.09±0.44)	13.99 (14.46±0.59)
GBM thickness (nm)	148.2 (151.3±8.7)	198.3 (195.6±9.6)[a]	165.3 (168.0±6.6)	240.6 (239.3±10.4)[c]

Data are expressed as the median and (the mean ± SE)
[a] different from 12W C, $p<0.01$, [b] different from 12W C, $p<0.05$, [c] different from 24W C, $p<0.01$, [d] different from 24W C, $p<0.05$

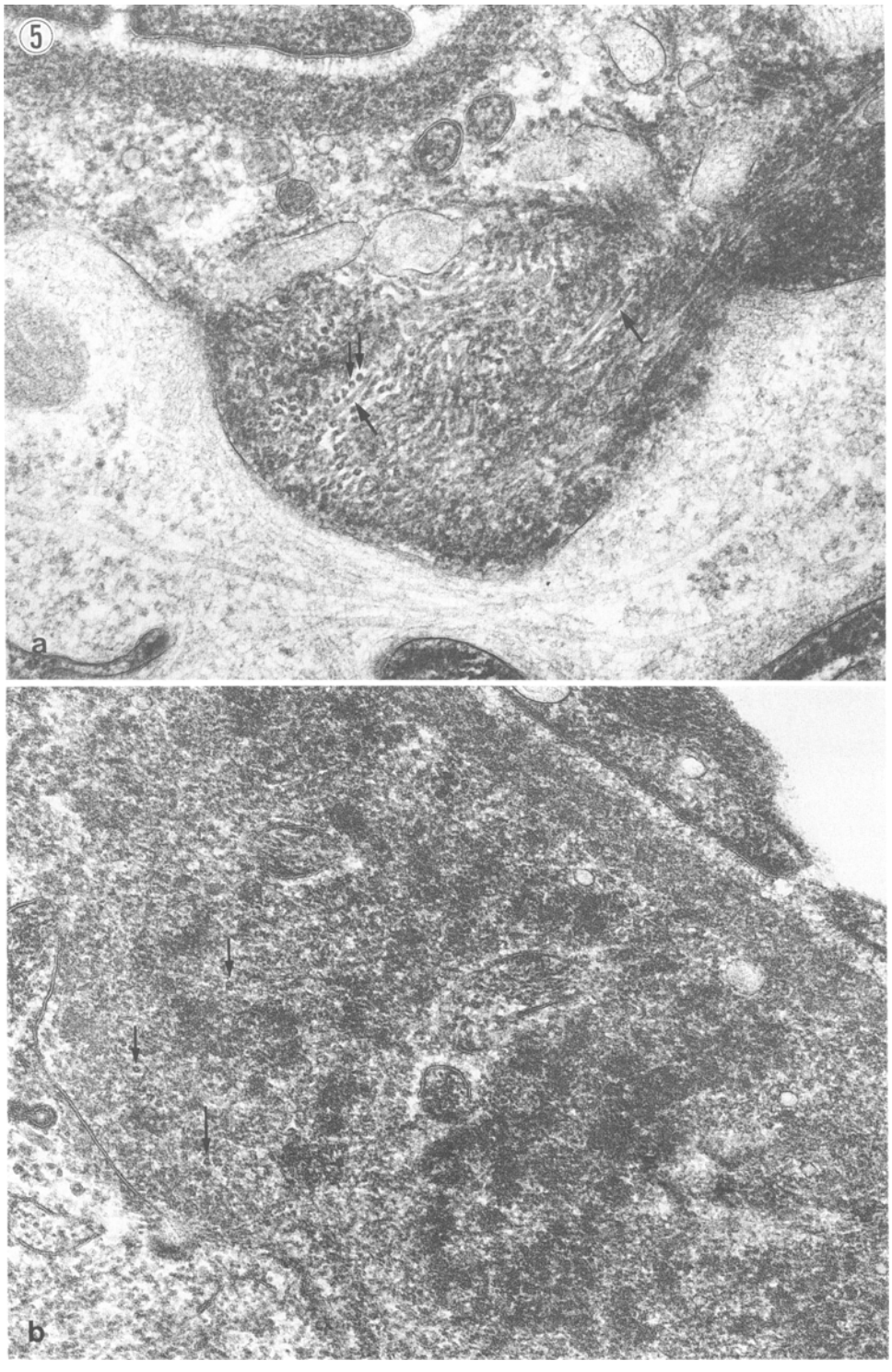

Fig. 5a, b. A high power view of the axial region of the mesangium in (**a**) the control and (**b**) 24 week diabetic rat. **a** The mesangial matrix in the control rat is made up of a network of microfibrils which are seen as longitudinal- (*large arrows*) and cross-sectional (*small arrows*) profiles. **b** In the diabetic rat, granular materials of heterogeneous density occupy most part of the mesangial matrix. Cross-sectional views of microfibrils (*arrows*) are scattered throughout these materials. TEM **a**, **b** ×75600

week and by 100% ($p<0.01$) in the 24 week duration diabetes. The distinct extension of the mesangial-capillary interface area made the capillary neck in the diabetics very wide.

Geometric changes which caused a moderate increase in the capillary volume were associated with an increase in the radius. The capillary diameter determined by assuming it had a cylindrical shape was increased by morphometric estimation (5%, $p<0.05$), in the 12 week and 5%, $p<0.05$, in the 24 week diabetics). The pericapillary GBM was thickened by 33% ($p<0.01$) in the 12 week and by 45% ($p<0.01$) in the 24 week diabetic rats.

Discussion

This study provided new findings by utilizing technical improvements in perfusion-fixation, in tissue processing,

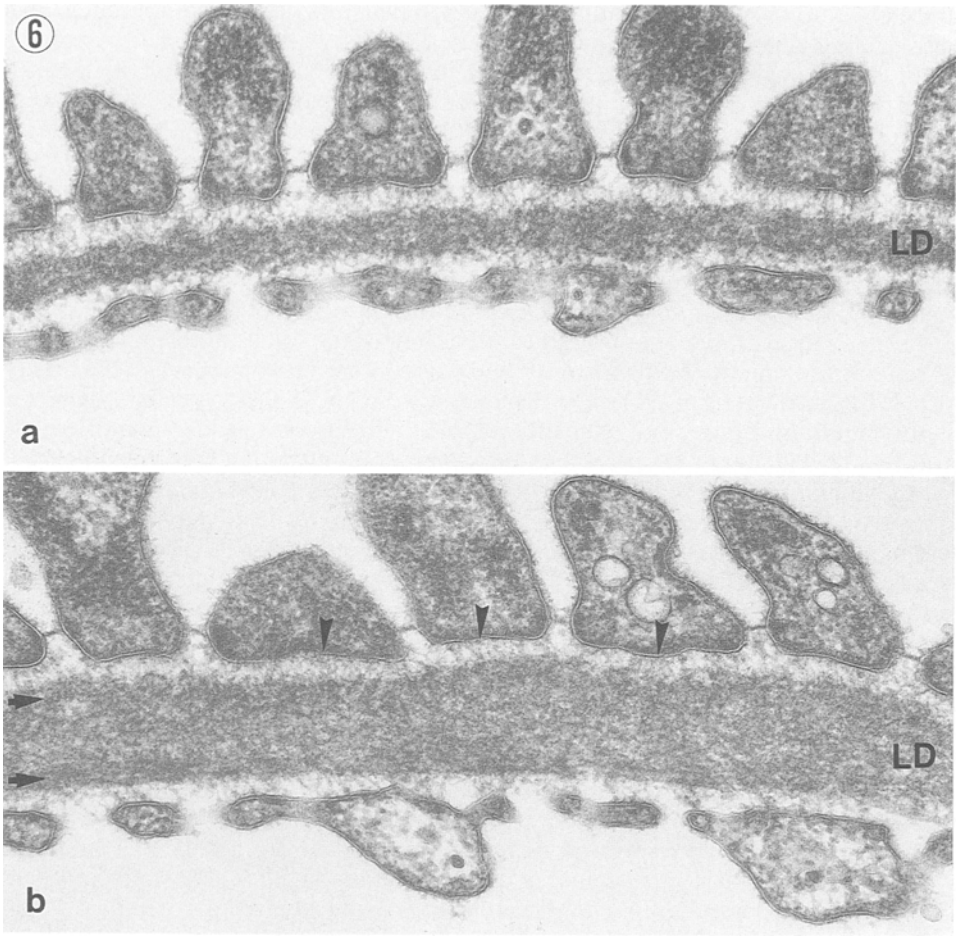

Fig. 6a, b. A high power view of a cross section of the peripheral GBM from a kidney of a (**a**) control and (**b**) 24 week diabetic rat. **a** The three layers of the GBM, namely the lamina rara interna, the lamina densa (*LD*), and the lamina rara externa, are clearly distinguished. In the laminae rarae, fine fibrils connect the lamina densa with the epithelial foot processes or with the endothelial cells. The lamina densa is composed of densely packed fibrogranular materials. **b** The GBM in diabetic rat is increased in thickness. The LD has dense sublayers (indicated by *arrows*) on both its epithelial and its endothelial side. Fine fibrils in the lamina rara externa (indicated by *arrowheads*) are more abundant than those in the control. TEM **a, b** ×75600

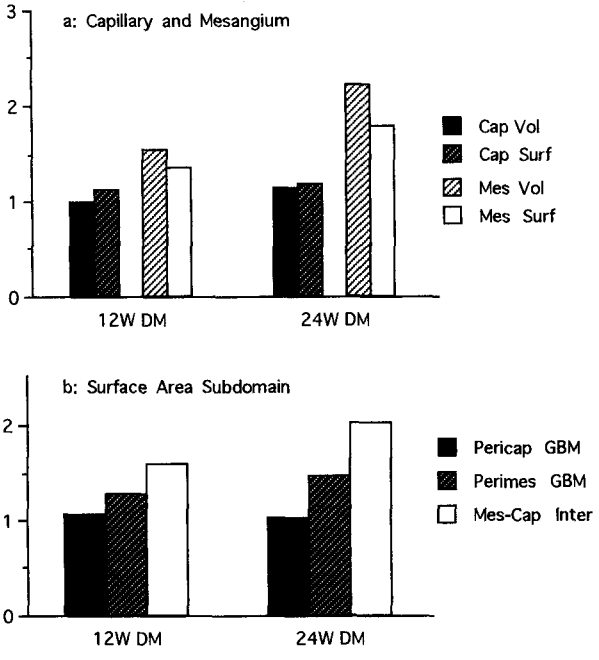

Fig. 7. Glomerular morphometric parameters expressed as relative values to control. Abbreviations: Cap Vol, Capillary Volume; Cap Surf, Capillary Surface Area; Mes Vol, Mesangial Volume; Mes Surf, Mesangial Surface Area; Pericap GBM, Pericapillary GBM Surface Area; Perimes GBM, Perimesangial GBM Surface Area; Mes-Cap Inter, Mesangial-Capillary Interface Surface Area

and in morphometry. Previous morphometric investigations have revealed several features of a diabetic glomerular lesion including an expansion of the mesangium and a thickening of the GBM (Steffes et al. 1980; Mauer et al. 1984, 1989; Østerby et al. 1988; Walker et al. 1992). However, these studies did not give an absolute estimate of the dimensional changes in individual compartments of the glomeruli and therefore did not allow one to understand the dynamics of the diabetic glomerular lesion.

We perfused the kidney with a pressure-control apparatus instead of by immersion-fixation. The glomerular geometry is controlled by a balance between the outward push of the blood pressure and the inward pull of mesangial contraction. In immersion-fixation, which fixes glomeruli at decreased blood pressure, the glomeruli are usually collapsed by active and elastic contraction of the mesangium and the GBM, which results in a decreased glomerular volume and an altered geometry. With perfusion-fixation using a perfusion pressure at the aorta approximately 50 mm Hg above the mean arterial pressure the glomerular volume remains almost constant (Miller and Meyer 1990). We operated the pressure-control apparatus at a pressure of 220 mm Hg, which was the minimal pressure necessary to fix the glomeruli without collapse in a preliminary study.

In processing the kidney tissue for transmission elec-

tron microscopy we employed a cold dehydration technique which minimizes treatment with osmium tetroxide and increases contrast with tannic acid and uranyl acetate (Sakai and Kriz 1987). With this procedure, the extra- and intracellular filamentous structures were preserved much better than with standard methods. Fine structures of the mesangial matrix and the GBM in the diabetic glomeruli were visualized in this study much more clearly than in previous studies.

Our morphometric approach tried to estimate the absolute sizes of various sub-domains of normal and diabetic glomeruli, according to the approach of Elger et al. (1990) and Sakai et al. (1992). Previous morphometric studies on diabetic glomeruli reported absolute values for only a few variables and did not provide the absolute values of the sub-domains systematically. This is necessary in order to understand fully the dynamics of the diabetic glomerular lesion.

We visualized the expanded mesangial matrix seen in diabetic rats and found that it was composed of a network of microfibrils and an accumulation of dense granular material. The accumulated granular material is rarely found in normal mesangium. It may represent either deposition of circulating macromolecules or an abnormally increased extracellular matrix. Evidence favouring the first possibility comes from immunohistochemical identification of immunoglobulin and complement in diabetic glomeruli (Tisher and Hostetter 1989). Non-enzymatic glycosylation of structural and circulating proteins might facilitate this deposition (Ziyadeh et al. 1989). Evidence for the second possibility comes from studies showing increased production and reduced degradation of the extracellular matrix (Ziyadeh et al. 1989). An altered composition of structural proteins in the diabetic mesangial matrix is indicated by immunohistochemical studies (Kim et al. 1991; Nerlich and Schleicher 1991).

Increased thickness of the GBM is one of the characteristic lesions in diabetic glomeruli. Both heterogeneous density in the lamina densa and increased fine fibrils in its lamina rara externa have been visualized for the first time in this study. These findings are compatible with previous immunohistochemical and biochemical studies which indicate compositional changes in the diabetic GBM (Kim et al. 1991; Nerlich and Schleicher 1991). These structural alterations in the diabetic GBM might be in part the basis of the increased permeability of circulating macromolecules in the diabetic glomerular capillary wall.

Enlargement of the mesangium typical of the diabetic glomeruli was associated with disproportionate enlargement of various sub-domains of the glomeruli which were analysed in detail in the present study. In the diabetic glomeruli the mesangial-capillary interface area had increased dramatically, the perimesangial GBM area had increased slightly and the pericapillary GBM area remained almost unchanged. These geometric changes may be summarized as a widening of the capillary neck associated with enlargement of the mesangium.

The degree of widening of the capillary neck in experimental models of glomerulopathy has been estimated quantitatively. A similar morphometric approach providing an absolute estimate of the sub-domain areas has been undertaken in the sub-acute adaptation of glomerular geometry to volume expansion and dehydration (Elger et al. 1990) and in glomerular failure in the isolated perfused kidney (Sakai et al. 1992). However, these studies did not provide evidence for an enlarged mesangial-capillary interface area. In the former study, the mesangial-capillary interface area was not measured. In the latter study, the interface area had a tendency to increase with increased perfusion pressure, but the increase was not significant because of the small sample taken.

Østerby and co-workers (1990) reported that there was a tendency toward a larger mean capillary diameter in diabetic patients. The present study quantified the increase in the capillary radius in the diabetic glomeruli. The enlargement of the mesangial-capillary interface is shown to be the primary factor involved in the increase of the capillary radius in the diabetics, whereas the pericapillary GBM area was almost unchanged. This geometric change represents a widening of the capillary neck. In a recent article on glomerular structure and dynamics, Kriz and co-workers (1990) proposed that capillaries with a wide neck represent the first sign of structural damage to the glomerular tuft. It is probable that the widening of the capillary neck in the diabetic glomeruli may have been brought about by haemodynamic changes such as increased glomerular capillary flow and pressure (Zatz et al. 1985) or by decreased contractile response of diabetic mesangial cell (Kikkawa et al. 1986).

Our present study showed that the capillaries had widened due to enlargement of the mesangial-capillary interface, which would be significant as a step in the progression of diabetic glomerulopathy. The enlargement of the mesangial-capillary interface area may increase the delivery of plasma protein to the mesangium and may in part be responsible for mesangial accumulation of macromolecules. Since filtration at the mesangial-capillary interface is non-selective (Michael et al. 1980), plasma proteins will be delivered to the mesangium in quantities proportional to the filtration surface area, that is to say the mesangial-capillary interface area. In diabetic glomeruli with a large capillary radius, the same transmural pressure differences causes more dilation of the capillary wall with a resultant high wall tension when compared with control glomeruli (LaPlace's law). On the basis of the ultrastructural geometry of the glomerulus, wall tension in the pericapillary GBM is thought to be transmitted to the mesangial cells through connections at mesangial angles (Sakai and Kriz 1987). It is interesting to note that increased mechanical stress on the cultured mesangial cells stimulates production of the extracellular matrix such as collagenous proteins (Harris et al. 1992).

Similar morphometric studies in other experimental models of glomerulopathy would elucidate to what degree the widening of the glomerular capillary necks may contribute to development of the mesangial widening in various kidney diseases.

Acknowledgements. The skillful technical assistance of Mr. Michio Murai, Mr. Mitsutaka Yoshida, Mr. Katsuhiro Sato, and Mr. Kouichi Igarashi is gratefully acknowledged.

References

Bankir L, Fischer C, Fischer S, Jukkala K, Specht HJ, Kriz W (1988) Adaptation of the rat kidney to altered water intake and urine concentration. Pflugers Arch 412:42–53

Elger M, Sakai T, Kriz W (1990) Role of mesangial cell contraction in adaptation of the glomerular tuft changes in extracellular volume. Pflugers Arch 415:598–605

Fujiwara CK, Padilha RM, Zatz R (1992) Glomerular abnormalities in long-term experimental diabetes: role of hemodynamic and nonhemodynamic factors and effects of antihypertensive therapy. Diabetes 41:286–293

Harris RC, Haralson MA, Badr KF (1992) Continuous stretch-relaxation in culture alters rat mesangial, morphology, growth characteristics, and metabolic activity. Lab Invest 66:548–554

Hirose K, Østerby R, Nazawa M, Jorgensen H, Gunderson G (1982) Development of glomerular lesions in experimental long-term diabetes in the rat. Kidney Int 21:689–695

Hyvarinen A, Nikkila EA (1962) Specific determination of blood glucose with *o*-toluidine. Clin Chim Acta 7:140–143

Kaissling B, Kriz W (1982) Variability of intercellular spaces between macula densa cells: a transmission electron microscopic study in rabbits and rats. Kidney Int 22:S9–S17

Kikkawa R, Kitamura E, Fujiwara Y, Arimura T, Haneda M, Shigeta Y (1986) Impaired contractile responsiveness of diabetic glomeruli to angiotensin II: a possible indication of mesangial dysfunction in diabetes mellitus. Biochem Biophys Res Comm 136:1185–1190

Kim Y, Kleppel MM, Butkowski R, Mauer SM, Wieslamder J, Michael AF (1991) Differential expression of basement membrane collagen chain in diabetic nephropathy. Am J Pathol 138:413–420

Kriz W, Elger M, Lemley KV, Sakai T (1990) Mesangial cell-glomerular basement membrane connections counteract glomerular capillary and mesangial enlargement. Am J Nephrol 10:S4–S13

Mauer SM, Steffes MW, Brown DM (1981) The kidney in diabetes. Am J Med 70:603–612

Mauer SM, Steffes MW, Ellis EN, Sutherland DER, Brown DM, Goetz F (1984) Structural-functional relationships in diabetic nephropathy. J Clin Invest 74:1143–1155

Mauer SM, Steffes MW, Azar S, Brown DM (1989) Effects of sorbinil on glomerular structure and function in long-term-diabetic rats. Diabetes 38:839–846

Michael AF, Keane WF, Raij L, Vernier RL, Mauer SM (1980) The glomerular mesangium. Kidney Int 17:141–154

Miller PL, Meyer TW (1990) Effects of tissue preparation on glomerular volume and capillary structure in the rat. Lab Invest 63:862–866

Nakamura T, Ebihara I, Shirato I, Tomino Y, Koide H (1991) Modulation of basement membrane component gene expression in glomeruli of aminonucleoside nephrosis. Lab Invest 64:640–647

Nerlich A, Schleicher E (1991) Immunohistochemical localization of extracellular matrix components in human diabetic glomerular lesions. Am J Pathol 139:889–899

Østerby R, Parving H-H, Nyberg G, Hommel E, Jørgensen HE, Lokkegaard H, Svalander C (1988) A strong correlation between glomerular filtration rate and filtration surface in diabetic nephropathy. Diabetologia 31:265–270

Østerby R, Parving H-H, Hommel E, Jørgensen HE, Lookegaard H (1990) Glomerular structure and function in diabetic nephropathy. Diabetes 39:1057–1063

Sakai T, Kriz W (1987) The structural relationship between mesangial cells and basement membrane of the renal glomerulus. Anat Embryol (Berl) 176:373–386

Sakai T, Lemley KV, Hackenthal E, Nagata M, Nobiling R, Kriz W (1992) Changes in glomerular structure following acute mesangial failure in the isolated perfused kidney. Kidney Int 41:533–541

Steffes MW, Brown DM, Basgen JM, Mauer SM (1980) Amelioration of mesangial volume and surface alterations following islet transplantation in diabetic rats. Diabetes 29:509–515

Tisher CC, Hostetter TH (1989) Diabetic nephropathy. In: Tisher CC, Brenner BM (eds) Renal pathology. Lippincott, Philadelphia, pp 1309–1334

Walker JD, Close CF, Jones S, Rafftery M, Keen H, Viberti GC, Østerby R (1992) Glomerular structure in type-1 (insulin-dependent) diabetic patients with normo- and microalbuminuria. Kidney Int 41:741–748

Weibel ER (1979) Stereological methods. Practical methods for biological morphometry. Academic Press, London

Zatz R, Meyer TW, Rennke HG, Brenner BM (1985) Predominance of hemodynamic rather than metabolic factors in the pathogenesis of diabetic glomerulopathy. Proc Natl Acad Sci USA 82:5963–5967

Ziyadeh FN, Goldfarb S, Kern EFO (1989) Diabetic nephropathy: metabolic and biochemical mechanisms. In: Brenner B, Stein JH (eds) The kidney in diabetes mellitus. Churchill Livingstone, New York, pp 87–113